Electronic Supplementary Information

Crystal phase engineering of Ru for simultaneous selective photocatalytic oxidations and H_2 production

Michaël Gebruers,[a, 1] Chunhua Wang,[b, 1] Rafikul A. Saha,[a] Yangshan Xie,[a] Imran Aslam,[a] Li Sun,[b] Yuhe Liao,[c] Xuhui Yang,[d] Taoran Chen,[d] Min-Quan Yang,[d] Bo Weng[a *] and Maarten B. J. Roeffaers[a *]

[a] *cMACS, Department of Microbial and Molecular Systems, KU Leuven, Celestijnenlaan 200F, 3001 Leuven, Belgium.*

[b] *Department of Chemistry, KU Leuven, Celestijnenlaan 200F, 3001 Leuven, Belgium*

[c] *Guangzhou Institute of Energy Conversion, Chinese Academy of Sciences, No. 2, Nengyuan, Road, Tianhe District, Guangzhou 510641, P.R. China.*

[d] *College of Environmental Science and Engineering, Fujian Key Laboratory of Pollution Control & Resource Reuse, Fujian Normal University, Fuzhou 350007, P.R. China*

[1] *These authors contributed equally to this work.*

** Corresponding author:*

E-mail: bo.weng@kuleuven.be; maarten.roeffaers@kuleuven.be

1. Supplementary figures and tables

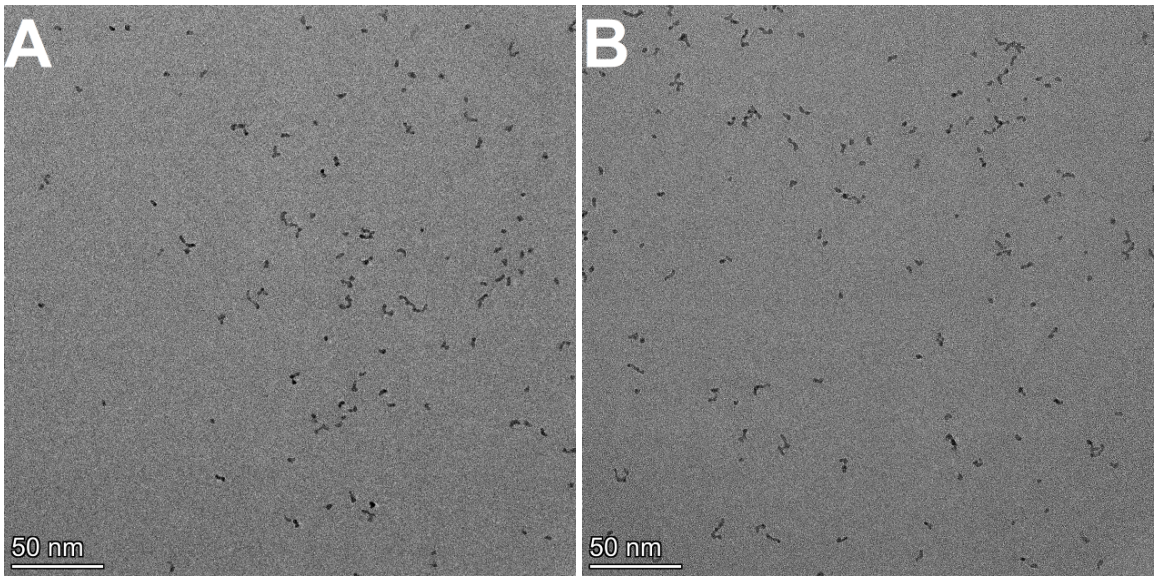

Fig. S1 TEM images of (A) fcc Ru NPs and (B) hcp Ru NPs.

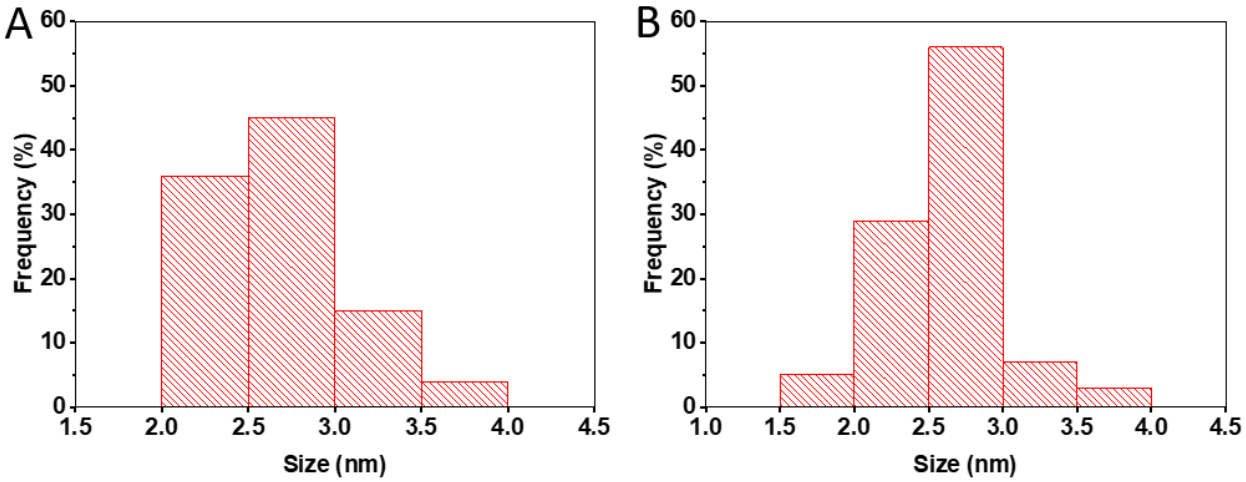

Fig. S2 Histograms showing the particle size distribution of (A) fcc Ru NPs and (B) hcp Ru NPs. The particle size was determined by measuring TEM images using ImageJ (50 particles measured).

Table S1 Amount of Ru loading of the Ru/TiO_2 composites determined via WDXRF.

Sample	Wt% Ru
0.15 wt% fcc-Ru/TiO_2	0.151 ± 0.014
0.30 wt% fcc-Ru/TiO_2	0.302 ± 0.027
0.60 wt% fcc-Ru/TiO_2	0.584 ± 0.038
0.90 wt% fcc-Ru/TiO_2	0.886 ± 0.068
1.20 wt% fcc-Ru/TiO_2	1.210 ± 0.029
0.60 wt% hcp-Ru/TiO_2	0.613 ± 0.012

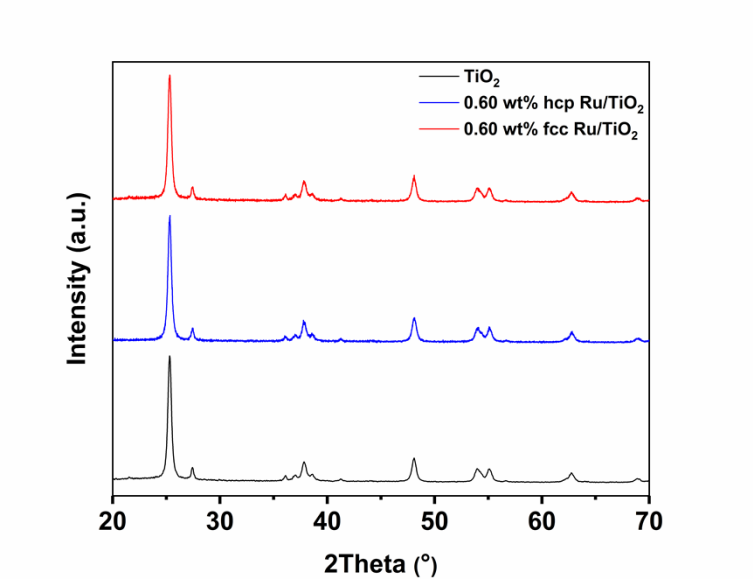

Fig. S3 XRD patterns of TiO_2, 0.60 wt% hcp Ru/TiO_2 and 0.60 wt% fcc Ru/TiO_2 composites.

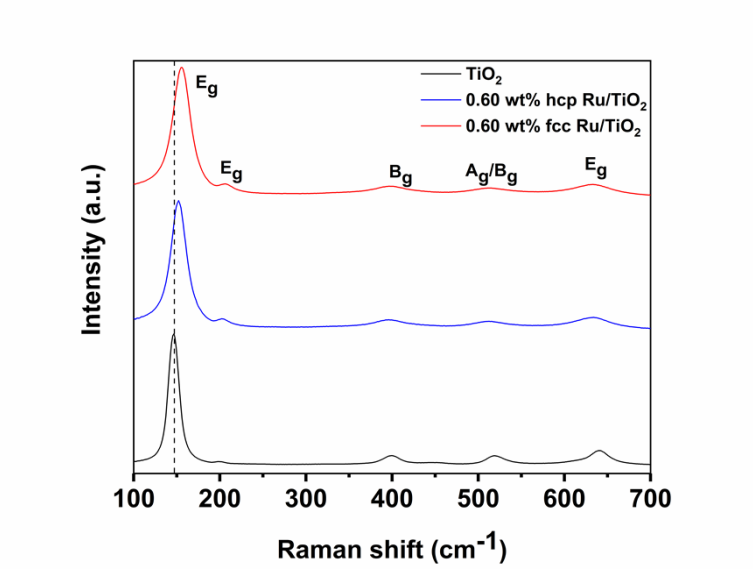

Fig. S4 Raman spectra of TiO_2, 0.60 wt% hcp Ru/TiO_2 and 0.60 wt% fcc Ru/TiO_2 composites.

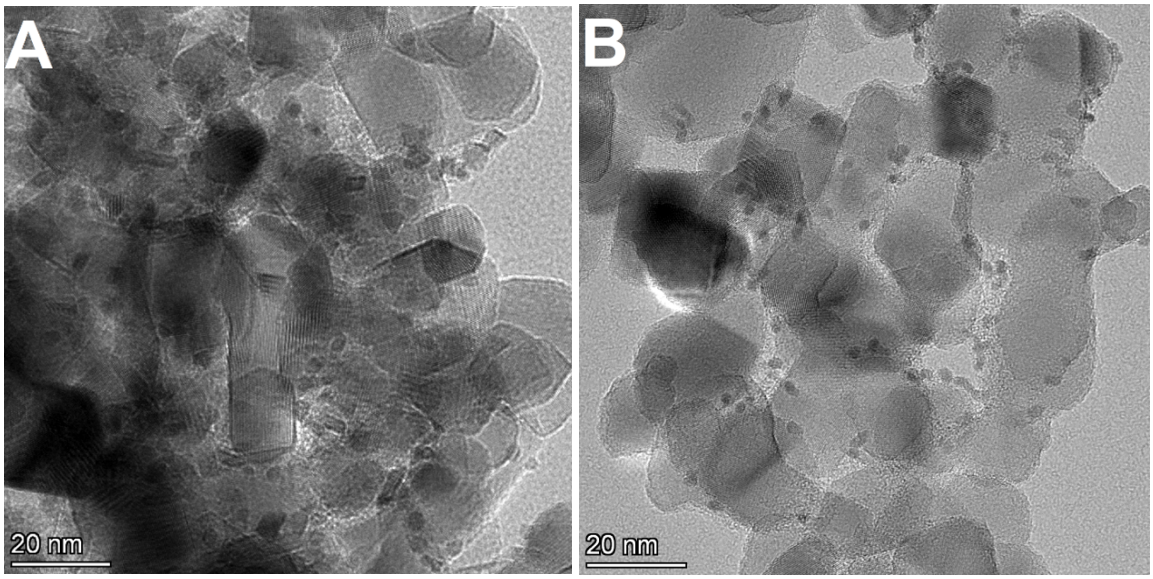

Fig. S5 TEM images of (A) 0.60 wt% fcc Ru/TiO_2 and (B).0.60 wt% hcp Ru/TiO_2.

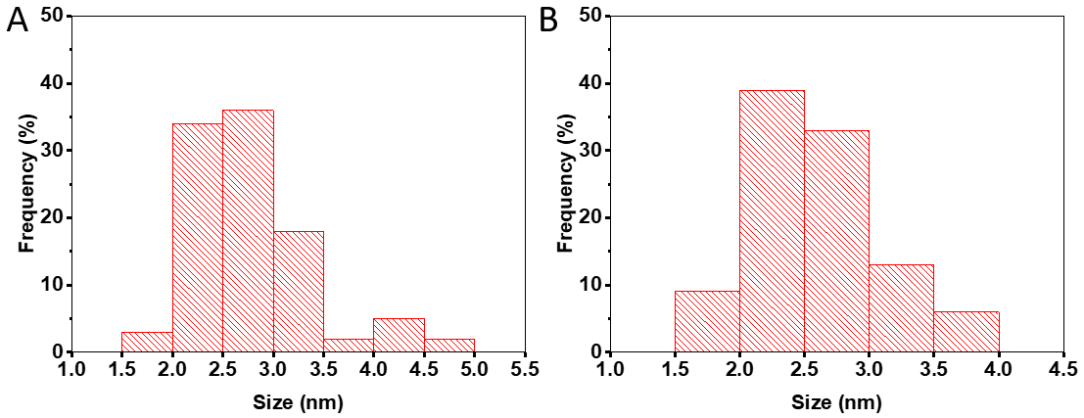

Fig. S6 Histograms showing the particle size distribution of (A) fcc Ru NPs and (B) hcp Ru NPs. The particle size was determined by measuring TEM images using ImageJ (40 particles measured).

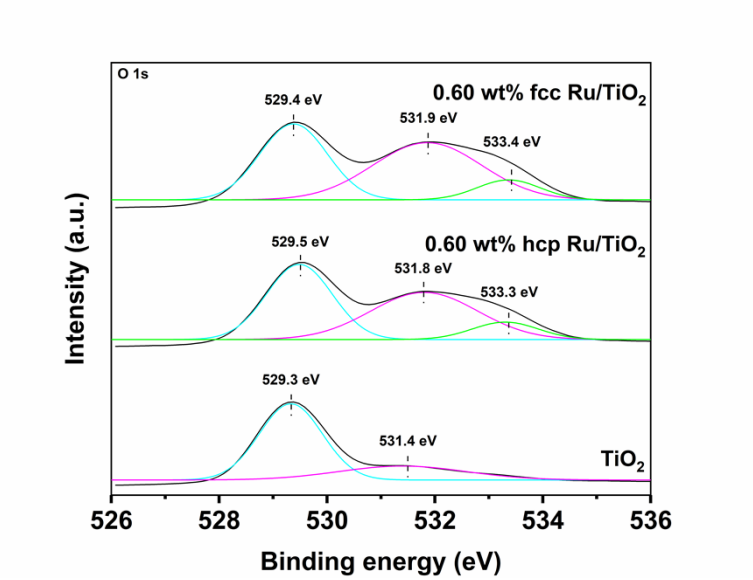

Fig. S7 Typical high-resolution XPS spectra of the core levels of O1s in different samples.

Note: The peaks located at ca. 533.3eV may originated from the residual PVP in the Ru NPs.[1]

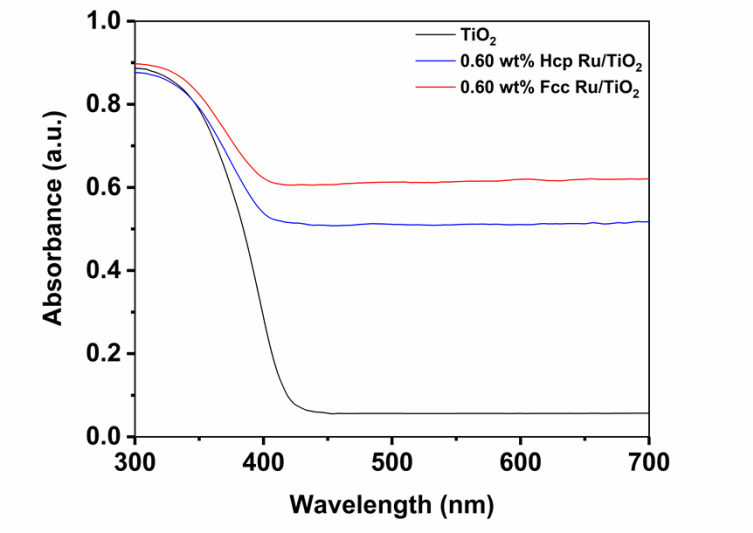

Fig. S8 DRS spectra of the TiO_2 and different Ru/TiO_2 composites

Calculation of the BAD and H_2 production rate

Calibration curves were generated for both BAD and H_2, these were used to determine the production rates in the photocatalytic conversion of BA to BAD and H_2. For the BAD calibration curve, a dilution series of BAD in trifluorotoluene with a total volume of 2.604 mL was prepared, which is the same volume as the total reaction volume and measured with gas chromatography (GC) (Shimadzu 2010 GC, CP-Sil 5, FID detector). This allows for the calibration curve to be used directly to calculate the amount of BAD formed in our catalysis experiments, without recalculating for the amount of solvent in the reaction. For H_2 various volumes of H_2 were injected directly in the GC (Shimadzu 2014 GC, molecular sieve 5A column, TCD detector) to generate the H2 calibration curve.

This resulted in the following formulas to calculate the amount of product formed:

$$n_{BAD}\ (\mu mol) = \frac{Signal\ (counts) + 43685\ (counts)}{39309\ (counts\ \mu mol^{-1})}$$

$$n_{H_2}\ (\mu mol) = \frac{Signal\ (counts) - 73\ (counts)}{5778\ (counts\ \mu mol^{-1})}$$

The production rate of H_2 and BAD was then calculated as follows:

$$Production\ rate\ (\mu mol\ g^{-1}\ h^{-1}) = \frac{n_{product}\ (\mu mol)}{m_{catalyst}\ (g) * t_{reaction}\ (h)}$$

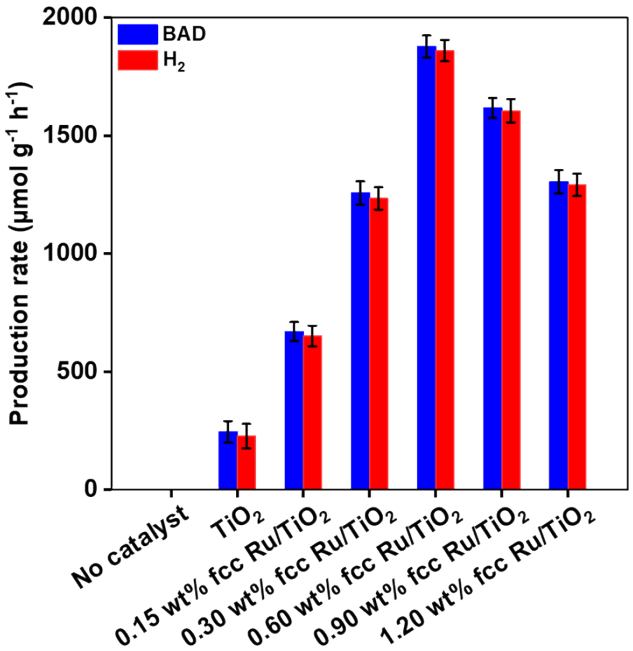

Fig. S9 Catalytic performance of TiO_2 and fcc Ru/TiO_2 with different amounts of Ru loading in the simultaneous photocatalytic benzaldehyde (BAD) and hydrogen production from benzyl alcohol. Reaction conditions: 1.0 mmol of benzyl alcohol, 15 mg of catalyst, 2.5 mL of trifluorotoluene, under vacuum, simulated solar light (300 W Xe lamp, AM 1.5 G), reaction time of 14h.

Table S2 Catalytic performance of TiO_2, fcc Ru/TiO_2 with different amounts of Ru loading and 0.60 wt% hcp Ru/TiO_2 in the simultaneous photocatalytic benzaldehyde (BAD) and hydrogen production from benzyl alcohol.

Catalyst	BAD production rate ($\mu mol\ g^{-1}\ h^{-1}$)	Hydrogen production rate ($\mu mol\ g^{-1}\ h^{-1}$)
No catalyst	0.0 ± 0.0	0.0 ± 0.0
TiO_2	245.5 ± 45.7	227.5 ± 51.3
0.15 wt% fcc Ru/TiO_2	670.1 ± 40.3	651.5 ± 44.0
0.30 wt% fcc Ru/TiO_2	1257.6 ± 48.9	1234.0 ± 47.4
0.60 wt% fcc Ru/TiO_2	1877.3 ± 46.5	1860.3 ± 45.2
0.90 wt% fcc Ru/TiO_2	1617.0 ± 42.6	1605.5 ± 49.1
1.20 wt% fcc Ru/TiO_2	1305.0 ± 49.1	1291.5 ± 47.0
0.60 wt% hcp Ru/TiO_2	1007.2 ± 50.5	986.5 ± 53.7

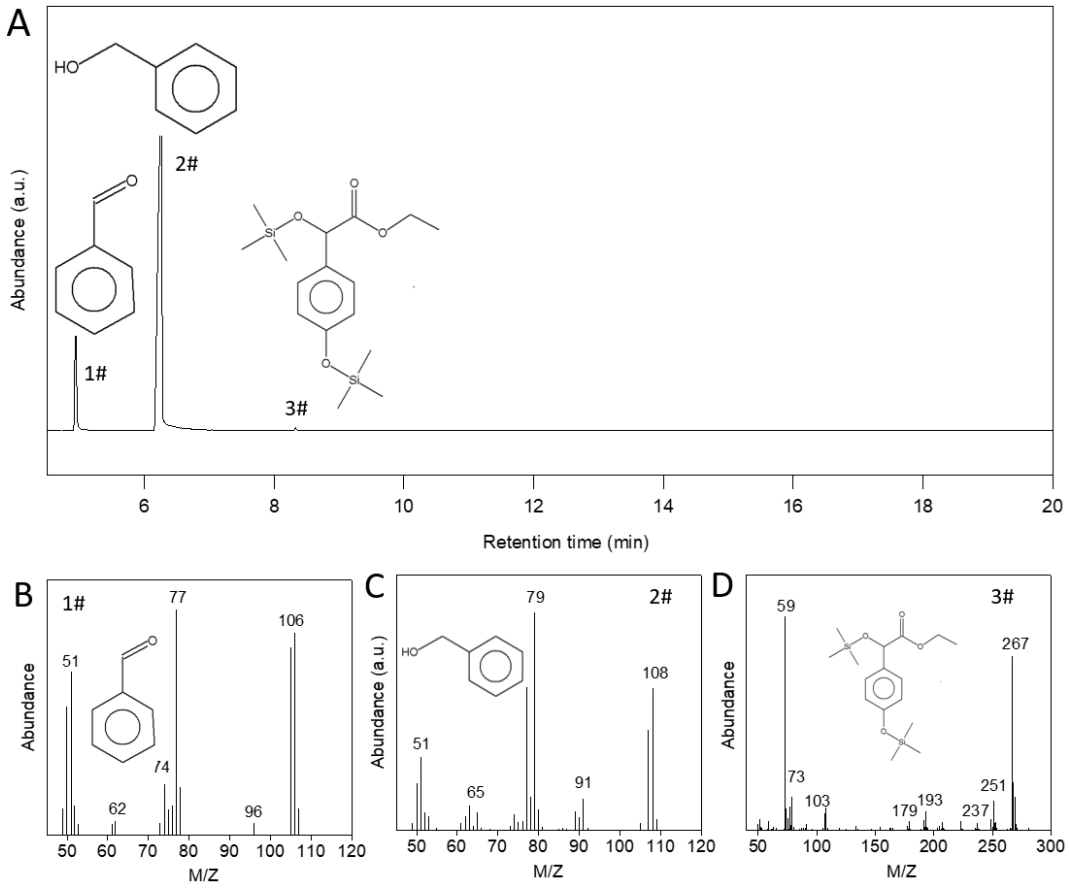

Fig. S10 GC-MS analysis of the products of the simultaneous benzaldehyde (BAD) and H_2 production from benzyl alcohol over 0.60 wt% fcc Ru/TiO_2 composite. Reaction conditions: 1.0 mmol of benzyl alcohol, 15 mg of catalyst, 2.5 mL of trifluorotoluene, under vacuum, simulated solar light (300 W Xe lamp, AM 1.5 G), reaction time of 14h.

Table S3 Recyclability of 0.60 wt% fcc Ru/TiO_2 in the simultaneous photocatalytic benzaldehyde (BAD) and hydrogen production from benzyl alcohol.

Cycle	BAD production rate	Hydrogen production rate

	(μmol g^{-1} h^{-1})	(μmol g^{-1} h^{-1})
1	1885.2 ± 54.8	1867.0 ± 51.4
2	1839.6 ± 53.3	1822.3 ± 52.0
3	1876.4 ± 46.9	1858.2 ± 44.5
4	1890.6 ± 45.5	1874.6 ± 49.6
5	1860.3 ± 47.3	1845.1 ± 46.3

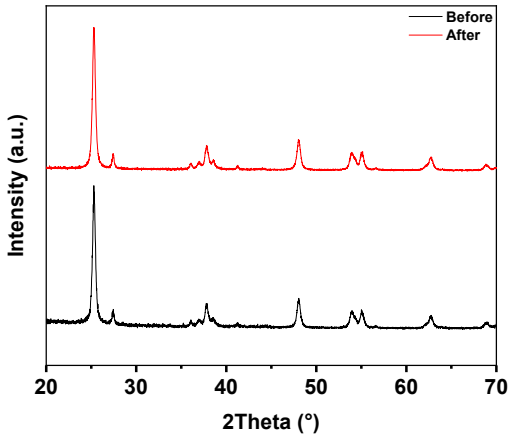

Fig. S11 XRD patterns of the 0.60 wt% fcc Ru/TiO_2 composite before and after catalytic reactions. Reaction conditions: 1.0 mmol of benzyl alcohol, 15 mg of catalyst, 2.5 mL of trifluorotoluene, under vacuum, simulated solar light (300 W Xe lamp, AM 1.5 G), reaction time of 14h.

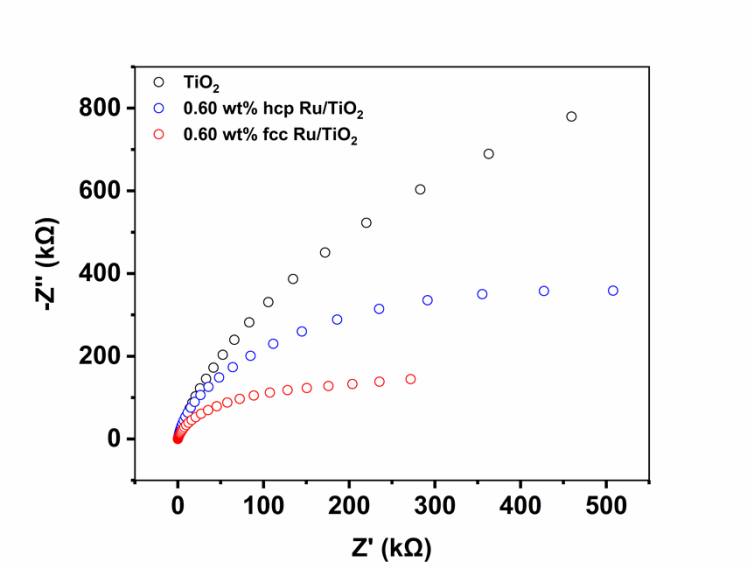

Fig. S12 Electrochemical impedance spectroscopy (EIS) spectra of the TiO_2, 0.60 wt% hcp Ru/TiO_2 and 0.60 wt% fcc Ru/TiO_2 composites.

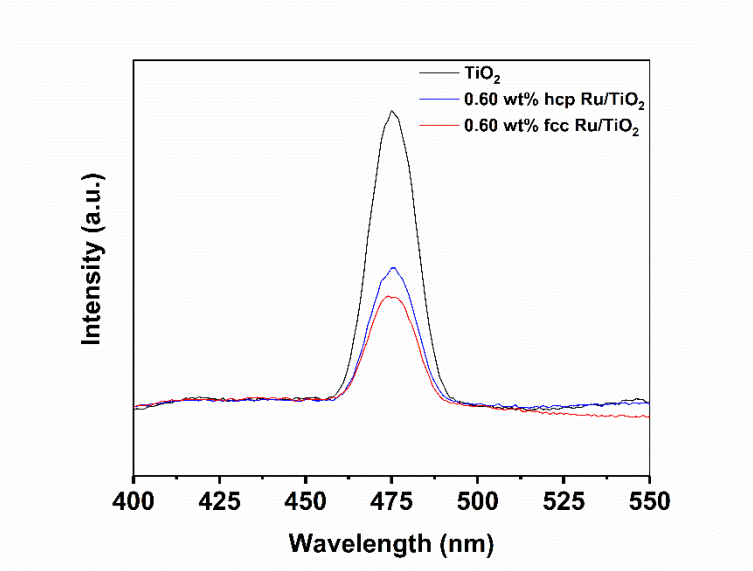

Fig. S13 Steady-state PL spectra of the TiO_2, 0.60 wt% hcp Ru/TiO_2 and 0.60 wt% fcc Ru/TiO_2 composites.

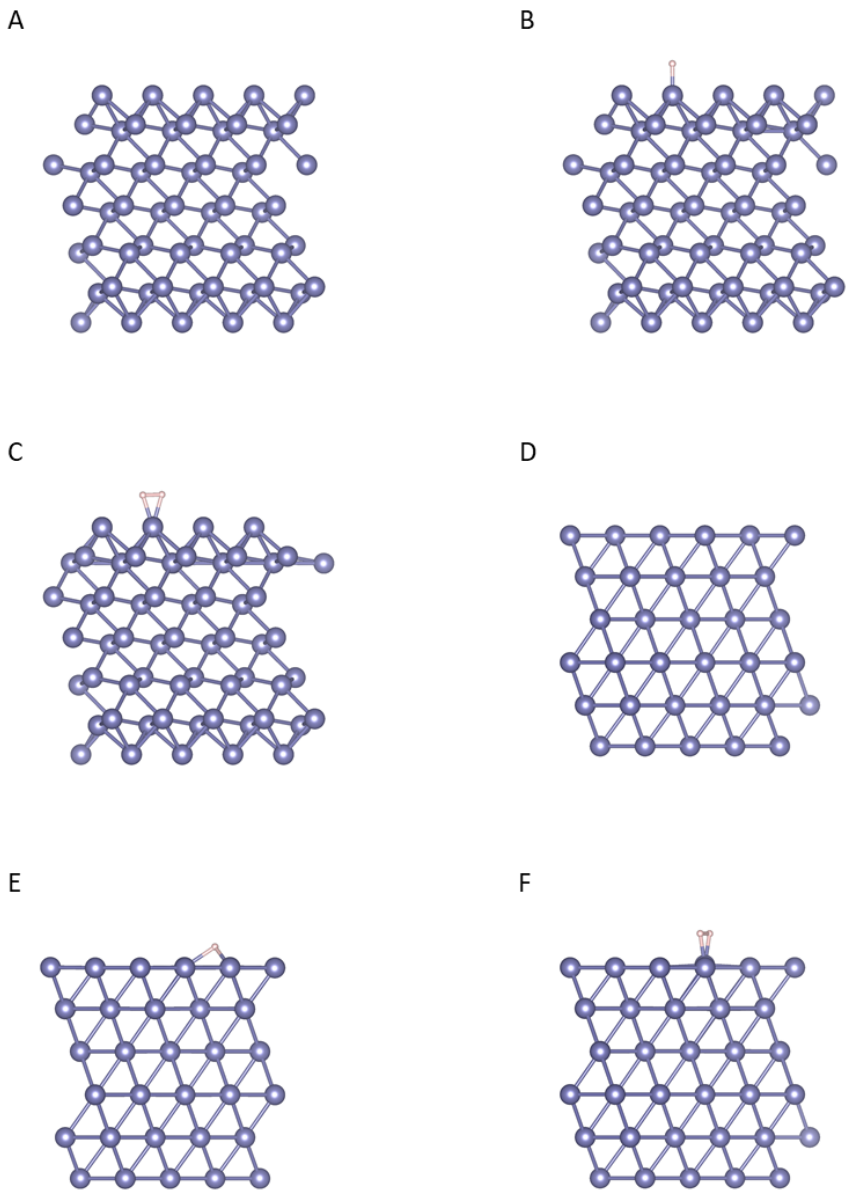

Fig. S14 Optimized structures calculated via DFT of (A) H(101) planes, (B) H^+ adsorbed on H(101) planes, (C) H_2 adsorbed on H(101) planes, (D) F(111) planes, (E) H^+ adsorbed on F(111) planes and (F) H_2 adsorbed on F(111) planes.

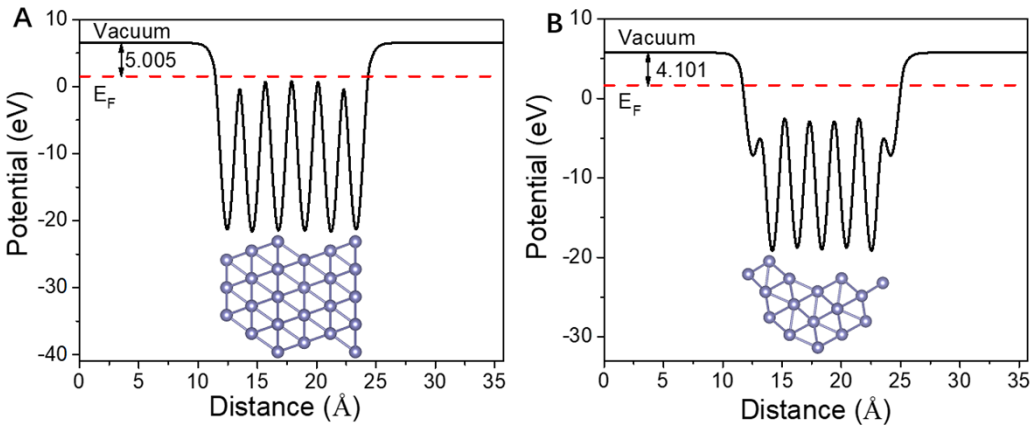

Fig. S15 The calculated electrostatic potential of (A) Ru F(111) and (B) Ru H(101) planes.

Table S4 Adsorption ability of H^+ and H_2 on the H(101) and F(111) planes of hcp and fcc Ru respectively, calculated via DFT.

Crystal plane	H^+ adsorption strength (eV)	H_2 adsorption strength (eV)
Hcp Ru – H(101)	-0.404	-0.680
Fcc Ru – F(111)	-0.621	-0.448

Calculation of Schottky barrier height:

The Schottky barrier height is calculated as follows:

$$\phi_b = \phi_{Ru} - X$$

In which ϕ_b the Schottky barrier height, ϕ_{Ru} is the work function of Ru and *X* the electron affinity of TiO_2. The work function (ϕ_{Ru}) of a surface model is usually obtained by calculating the electrostatic potential along the *z-axis*. It is defined as $\phi_{Ru} = E_O - E_F$, where E_O and E_F are the energy of vacuum level and the Fermi level, respectively. Therefore, the work functions of fcc and hcp Ru can be obtained from the DFT calculations as is shown in **Fig. S15**.

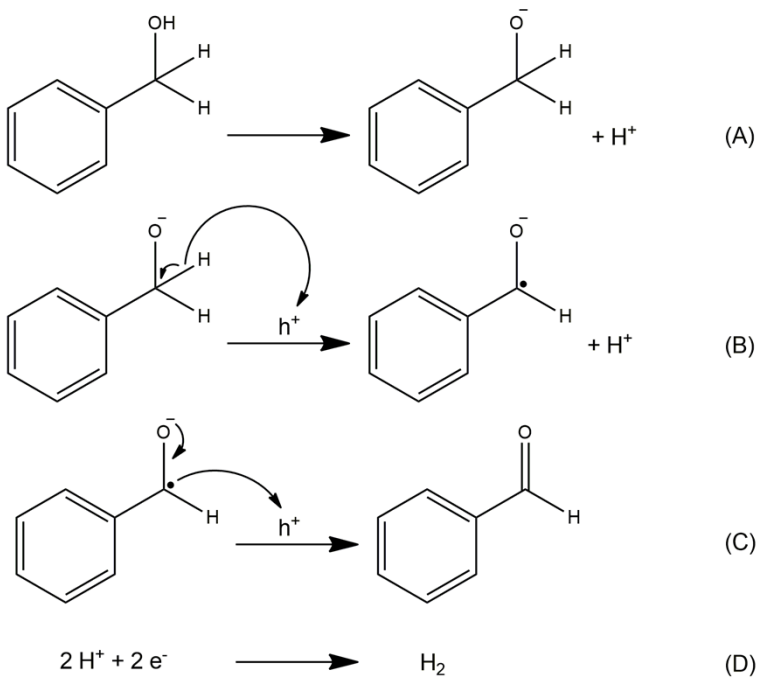

Scheme S1 Reaction mechanism for the simultaneous photocatalytic benzaldehyde (BAD) (A–C) and hydrogen production (D) from benzyl alcohol over Ru/TiO2 PCs.

Table S5 Catalytic performance of the 0.60 wt% fcc Ru/TiO_2 composite in different reaction conditions.

Different conditions	**BAD production rate ($\mu mol\ g^{-1}\ h^{-1}$)**	**Hydrogen production rate ($\mu mol\ g^{-1}\ h^{-1}$)**
No light	0.0 ± 0.0	0.0 ± 0.0
No catalyst	0.0 ± 0.0	0.0 ± 0.0

Table S6 Catalytic performance of the 0.60 wt% fcc Ru/TiO_2 composite in the absence of scavengers, in the presence of potassium persulfate as an electron scavenger and in the presence of ammonium oxalate as a hole scavenger in the simultaneous photocatalytic benzaldehyde (BAD) and hydrogen production from benzyl alcohol.

Scavenger	**BAD production rate ($\mu mol\ g^{-1}\ h^{-1}$)**	**Hydrogen production rate ($\mu mol\ g^{-1}\ h^{-1}$)**
No scavenger	1877.3 ± 46.5	1860.6 ± 45.2
Potassium persulfate	1831.2 ± 42.0	421.7 ± 51.2
Ammonium oxalate	315.3 ± 39.5	237.8 ± 53.5

3. References

1 S. Kang, R. C. Pawar, Y. Pyo, V. Khare and C. S. Lee, *J. Exp. Nanosci.*, 2016, **11**, 259–275.